



HAL
open science

Modeling (some aspects of) the female reproductive system

Romain Yvinec

► **To cite this version:**

Romain Yvinec. Modeling (some aspects of) the female reproductive system. Séminaire d'analyse appliquée A³, Laboratoire Amiénois de Mathématique Fondamentale et Appliquée, Oct 2021, Amiens, France. hal-03727263

HAL Id: hal-03727263

<https://hal.inrae.fr/hal-03727263v1>

Submitted on 19 Jul 2022

HAL is a multi-disciplinary open access archive for the deposit and dissemination of scientific research documents, whether they are published or not. The documents may come from teaching and research institutions in France or abroad, or from public or private research centers.

L'archive ouverte pluridisciplinaire **HAL**, est destinée au dépôt et à la diffusion de documents scientifiques de niveau recherche, publiés ou non, émanant des établissements d'enseignement et de recherche français ou étrangers, des laboratoires publics ou privés.

Modeling (some aspects of) the female reproductive system

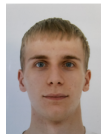
Romain Yvinec

Equipe BIOS, Physiologie de la Reproduction et des Comportements, INRAE
(Tours)

Equipe MUSCA, INRIA-INRAE-CNRS (Saclay)

Remerciement

- ★ INRIA Saclay : Frédérique Clément, Guillaume Ballif, Frédérique Robin
- ★ INRAE PRC : Team BIOS, BINGO (Danielle Monniaux, Véronique Cadoret, Rozenn Dalbies-Tran)
- ★ INRAE LPGP (Julien Bobe, Violette Thermes)
- ★ CEMRACS 2018 (Céline Bonnet (CMAP, X), Kerloum Chahour (U. Côte d'Azur))



Inria INRAE

Problèmes scientifiques et sociétaux en reproduction

Compréhension d'un processus complexe de biologie du développement, survenant pendant toute la durée de vie

- De nombreux types de cellules impliqués et diverses interactions
- De nombreuses échelles spatiales et temporelles différentes
- Rétroaction hormonale (endocrinienne, paracrine, autocrine)
- Contrainte stérique et biophysique

Préserver la capacité de reproduction

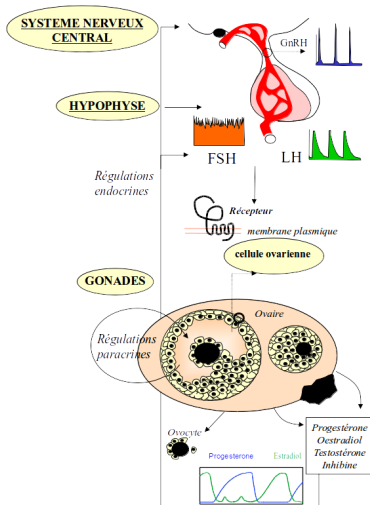
- Altérations iatrogènes ou physiologiques
- Sensibilité aux conditions environnementales
- Préservation de la biodiversité

Contrôle de la fonction de reproduction (chez l'Homme et l'animal)

- Biotechnologie de la reproduction (*in vivo*, *ex vivo*, *in vitro*)
- Enjeux clinique, économique et environnementaux

Le système reproducteur féminin des mammifères : un système multi-échelle complexe

- Signaux neuro-hormonaux
Encodage et décodage
- Gamétogenèse
Dynamique de population
- Croissance d'un follicule
Morphodynamique de cellules
- Niveau intra-cellulaire
réseaux de signalisation



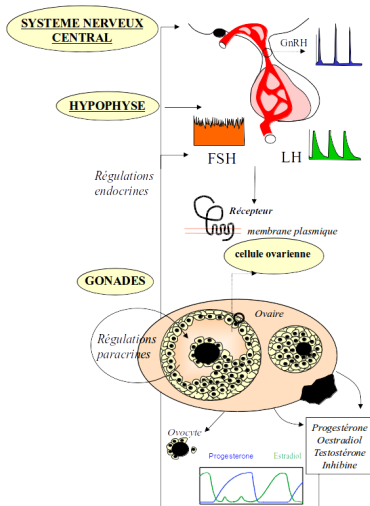
R.Y., P. Crépieux, E. Reiter, A. Poupon, F. Clément, *Advances in computational modeling approaches of pituitary gonadotropin signaling*, Expert Opinion on Drug Discovery, 2018.



F. Clément, P. Crépieux, R. Y., and D. Monniaux. Mathematical modeling approaches of cellular endocrinology within the hypothalamo-pituitary-gonadal axis. *Mol. Cell. Endocrinol.* 2020.

Le système reproducteur féminin des mammifères : un système multi-échelle complexe

- **Signaux neuro-hormonaux**
Encodage et décodage
- **Gamétogenèse**
Dynamique de population
- **Croissance d'un follicule**
Morphodynamique de cellules
- **Niveau intra-cellulaire**
réseaux de signalisation



R.Y., P. Crépieux, E. Reiter, A. Poupon, F. Clément, *Advances in computational modeling approaches of pituitary gonadotropin signaling*, Expert Opinion on Drug Discovery, 2018.



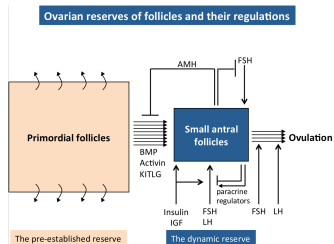
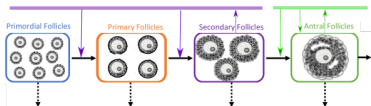
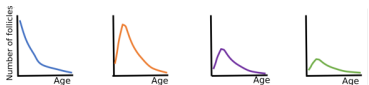
F. Clément, P. Crépieux, R. Y., and D. Monniaux. Mathematical modeling approaches of cellular endocrinology within the hypothalamo-pituitary-gonadal axis. *Mol. Cell. Endocrinol.* 2020.

Le système reproducteur féminin des mammifères : un système multi-échelle complexe

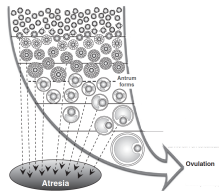
- **Gamétogenèse**

Dynamique de population

- Espace : niveau tissulaire
- Temps : vie reproductive

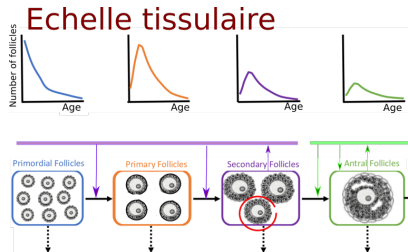


Monniaux, *Theriogenology* 2016

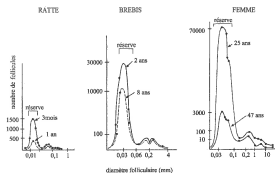
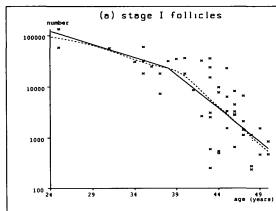


Scaramuzzi et al., *Reprod.Fert. Dev.* 2011

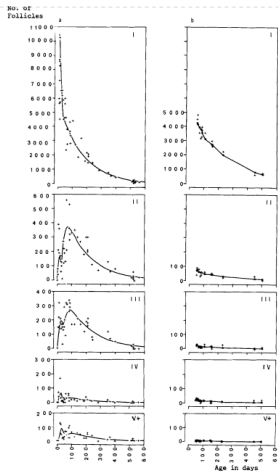
Modèles de population de follicules (vie reproductive)



- ⇒ Evolution irréversible d'un pool initial de follicule quiescent
- ⇒ Décroissance lente du nombre total de follicules et répartition "stable" dans l'espace de maturité (ou taille)



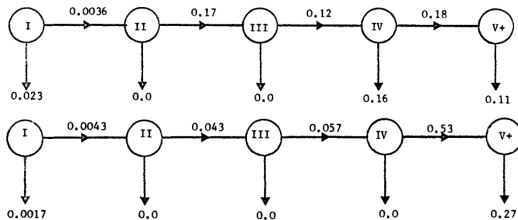
Modèles de population de follicules (vie reproductive)



An Analytical Model for Ovarian Follicle Dynamics

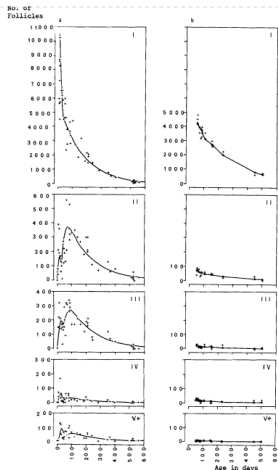
M. J. FADDY,¹ ESTHER C. JONES² AND R. G. EDWARDS³
¹ Department of Mathematical Statistics, University of Birmingham, Birmingham B15 2TT, U.K., ² Department of Anatomy, University of Birmingham, Birmingham B15 2TJ, U.K., and ³ Physiological Laboratory, University of Cambridge, Cambridge CB2 3EG, U. K.

- Modèle "migration-mort"
- Modèle linéaire inhomogène en temps



Faddy et al., J. Exp. Zool. 1976

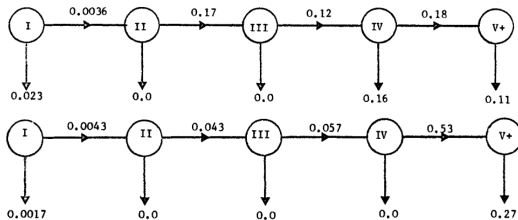
Modèles de population de follicules (vie reproductive)



An Analytical Model for Ovarian Follicle Dynamics

M. J. FADDY,¹ ESTHER C. JONES² AND R. G. EDWARDS³
¹Department of Mathematical Statistics, University of Birmingham, Birmingham B15 2TT, U.K., ²Department of Anatomy, University of Birmingham, Birmingham B15 2TJ, U.K., and ³Physiological Laboratory, University of Cambridge, Cambridge CB2 3EG, U. K.

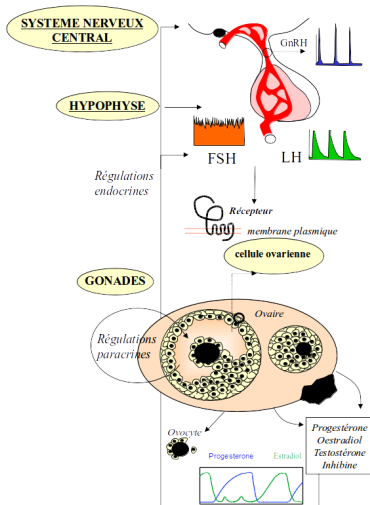
- Peut-on expliquer ces dynamiques avec des interactions non linéaire ?
- Quels paramètres peut-on inférer à partir de ces observations ?



Faddy et al., J. Exp. Zool. 1976

Le système reproducteur féminin des mammifères : un système multi-échelle complexe

- Signaux neuro-hormonaux
Encodage et décodage
- Gamétogenèse
Dynamique de population
- Croissance d'un follicule
Morphodynamique de cellules
- Niveau intra-cellulaire
réseaux de signalisation



R.Y., P. Crépieux, E. Reiter, A. Poupon, F. Clément, *Advances in computational modeling approaches of pituitary gonadotropin signaling*, Expert Opinion on Drug Discovery, 2018.



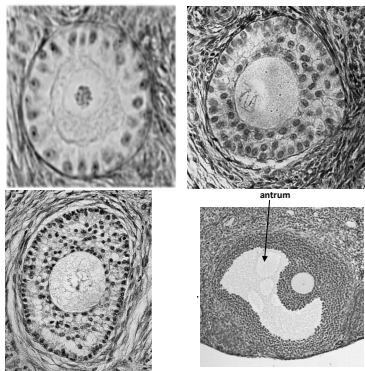
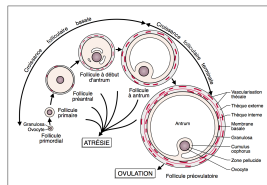
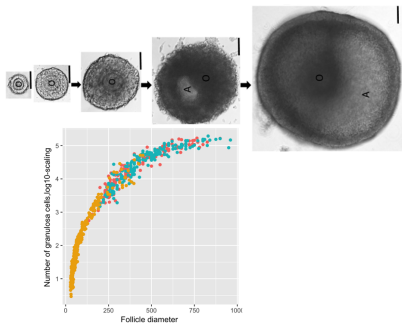
F. Clément, P. Crépieux, R. Y., and D. Monniaux. Mathematical modeling approaches of cellular endocrinology within the hypothalamo-pituitary-gonadal axis. *Mol. Cell. Endocrinol.* 2020.

Le système reproducteur féminin des mammifères : un système multi-échelle complexe

- **Croissance d'un follicule**

Morphodynamique de population

- Espace : niveau cellulaire
- Temps : Plusieurs cycles ovariens

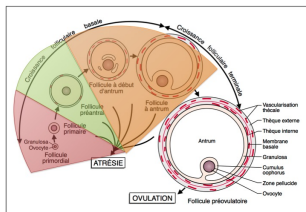


Courtesy of Danielle Monniaux.



Modélisation de la croissance d'un follicule

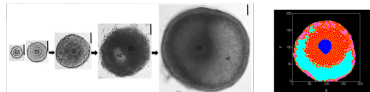
Croissance d'un follicule



Monniaux et al., M/S. 1999

- Thèse de F. Robin, (co-supervisée. F. Clément)

Echelle cellulaire



Différentes phases de croissance

- **Activation**
Transition / Prolifération cellulaire
- **Croissance Basale**
Prolifération / superposition cellulaire
- **Croissance Antrale**
Prolifération / Différentiation cellulaire et cavitation
- **Phase Terminale**
Prolifération / Différentiation et dépendance aux gonadotropines

Gametogenesis : Ovarian folliculogenesis

- Morphogenesis and maturation of ovarian follicles
 somatic and germ (egg) cells
 ⇒ Somatic cell division and germ cell growth up to ovulation

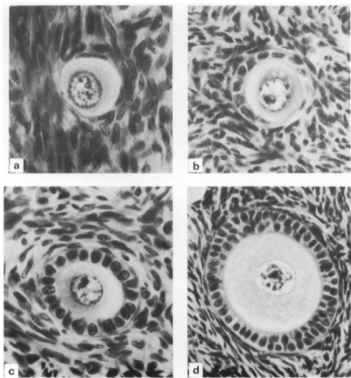
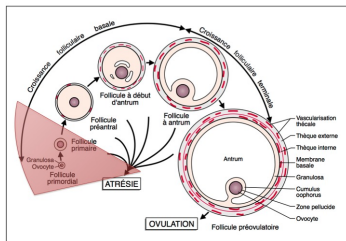


Fig. 1. Illustrations of follicle types: (a) Type B, $\times 570$; (b) Type B/C, $\times 570$; (c) Type C, $\times 570$; (d) Type D, $\times 410$.

Gougeon & Chainy, J. Reprod. Fert. 1987

Gametogenesis : Ovarian folliculogenesis

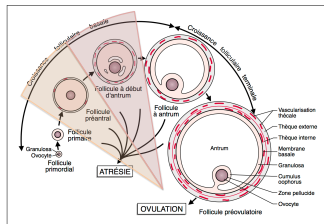
- Morphogenesis and maturation of ovarian follicles
somatic and germ (egg) cells
- Pool of Quiescent follicles
static reserve (perinatal in most mammals)
 Slow activation



Monniaux, *Theriogenology* 2016

Gametogenesis : Ovarian folliculogenesis

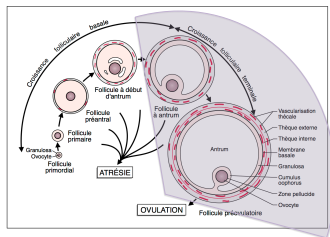
- Morphogenesis and maturation of ovarian follicles
somatic and germ (egg) cells
- Pool of Quiescent follicles
static reserve (perinatal in most mammals)
 Slow activation
- Basal growth
Dynamic reserve (starting at birth)
 Spanning over several ovarian cycles



Monniaux, Theriogenology 2016

Gametogenesis : Ovarian folliculogenesis

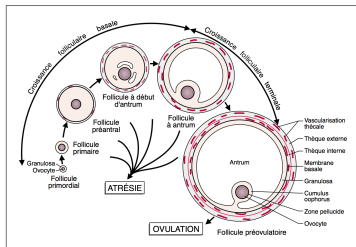
- Morphogenesis and maturation of ovarian follicles
 somatic and germ (egg) cells
- Pool of Quiescent follicles
 static reserve (perinatal in most mammals)
 Slow activation
- Basal growth
 Dynamic reserve (starting at birth)
 Spanning over several ovarian cycles
- Terminal growth
 After puberty : ovulation within an ovarian cycle



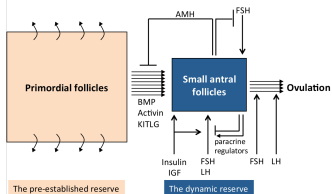
Monniaux, Theriogenology 2016

Gametogenesis : Ovarian folliculogenesis

- Morphogenesis and maturation of ovarian follicles
somatic and **germ** (egg) cells
- Pool of Quiescent follicles
static reserve (perinatal in most mammals)
 Slow activation
- Basal growth
Dynamic reserve (starting at birth)
 Spanning over several ovarian cycles
- Terminal growth
 After puberty : **ovulation** within an ovarian cycle
- Interactions between all follicles via complex (neuro-) hormonal signals



Ovarian reserves of follicles and their regulations



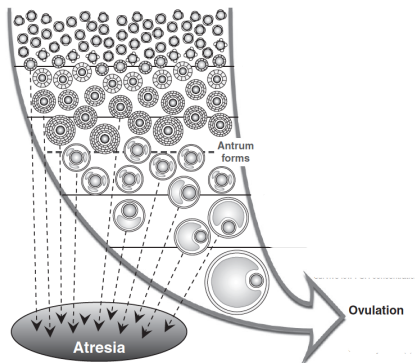
Monniaux, Theriogenology 2016

Order of magnitude

Follicle population in women

- Quiescent follicles

peri-natal	$\approx 5 \cdot 10^6$
At birth	$\approx 1 \cdot 10^6$
At puberty	$10^4 - 10^6$
At menopause	$< 10^3$
Activation rate	"A few per days"



Scaramuzzi et al., *Reprod.Fert. Dev.* 2011

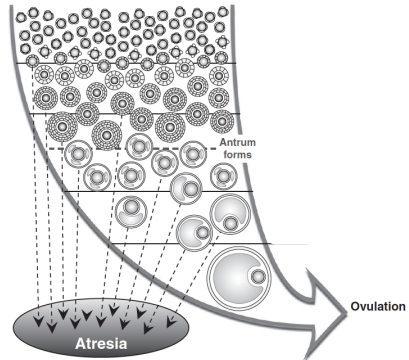
Order of magnitude

Follicle population in women

- Quiescent follicles

peri-natal	$\approx 5 \cdot 10^6$
At birth	$\approx 1 \cdot 10^6$
At puberty	$10^4 - 10^6$
At menopause	$< 10^3$
Activation rate	"A few per days"
- Growing follicles

Maturation time	120 – 180j
Basal follicles	$10^3 - 10^4$
Terminal follicles	10^2
Pre-Ovulatory follicles	a few
Atresia	Most of them !



Scaramuzzi et al., *Reprod.Fert. Dev.* 2011

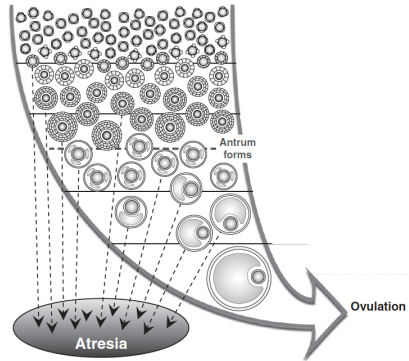
Order of magnitude

Follicle population in women

- Quiescent follicles

peri-natal	$\approx 5 \cdot 10^6$
At birth	$\approx 1 \cdot 10^6$
At puberty	$10^4 - 10^6$
At menopause	$< 10^3$
Activation rate	"A few per days"
 - Growing follicles

Maturation time	120 – 180j
Basal follicles	$10^3 - 10^4$
Terminal follicles	10^2
Pre-Ovulatory follicles	a few
Atresia	Most of them !
- > **Only 400 follicles will ever reach the pre-ovulatory stage**

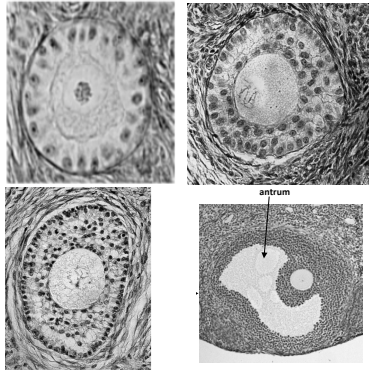


Scaramuzzi et al., *Reprod.Fert. Dev.* 2011

Order of magnitude

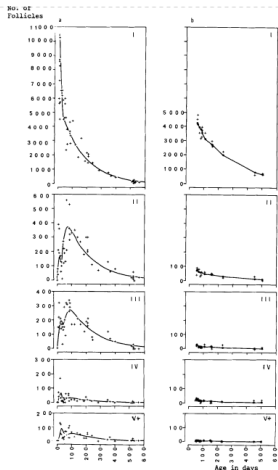
- a single follicle (in women)
 at different maturation stages

somatic cells diam.	$10\mu m$
ovocyte (egg cell) diam. :	$10 - 100\mu m$
follicle diam.	$0.03 - 20mm$
nb somatic cells	$10^2 - 10^7$



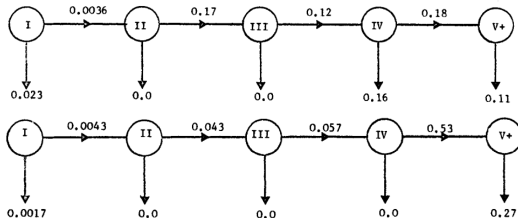
Courtesy of Danielle Monniaux.

Modèles de population de follicules (vie reproductive)



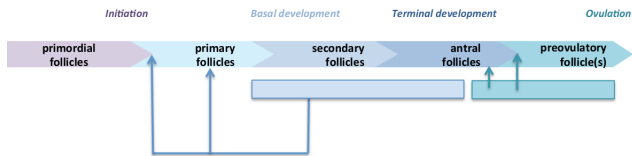
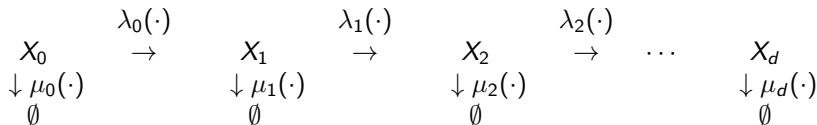
Faddy et al., J. Exp. Zool. 1976

- Peut-on expliquer ces dynamiques avec des interactions non linéaire ? Comment les analyser sur l'échelle de temps de vie d'un individu ?
- Quels paramètres peut-on inférer à partir de ces observations ?



Modèles de population de follicules (vie reproductive)

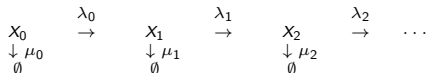
- Population structurée en compartiments
- Interaction non linéaire entre les populations de follicules via λ 's et μ 's.



Bonnet et al. *Multiscale population dynamics in reproductive biology : singular perturbation reduction in deterministic and stochastic models*, ESAIM : PROCEEDINGS AND SURVEYS, 2020.

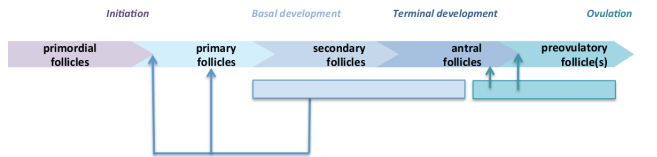
Modèles de population de follicules (vie reproductive)

- Population structurée en compartiments
- Interaction non linéaire entre les populations de follicules via λ 's et μ 's.



un choix possible

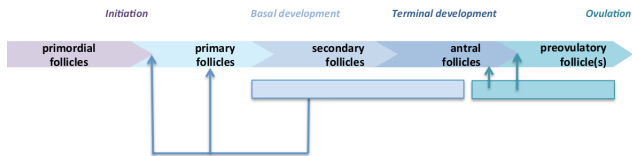
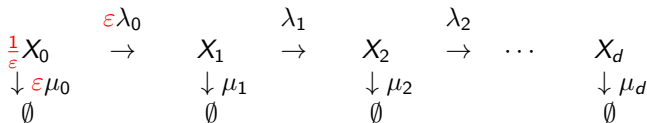
$$\begin{aligned}
 \lambda_i(X) &= m_i + \frac{f_i}{1 + K_{1,i} \sum_{j=0}^d \omega_{1,j} X_j}, \\
 \mu_i(X) &= g_i \left(1 + K_{2,i} \sum_{j=0}^d \omega_{2,j} X_j \right)
 \end{aligned}$$



Bonnet et al. *Multiscale population dynamics in reproductive biology : singular perturbation reduction in deterministic and stochastic models*, ESAIM : PROCEEDINGS AND SURVEYS, 2020.

Modèles de population de follicules (vie reproductive)

- Population structurée en compartiments
- Interaction non linéaire entre les populations de follicules via λ 's et μ 's.
- Deux échelles de temps/nombres
- Pool quiescent \gg Follicules en croissance
- Activation lente \ll croissance rapide



Bonnet et al. *Multiscale population dynamics in reproductive biology : singular perturbation reduction in deterministic and stochastic models*, ESAIM : PROCEEDINGS AND SURVEYS, 2020.

Chaîne de Markov en temps continu, remise à l'échelle :
 $(X^\varepsilon(t) = \varepsilon X_0(t/\varepsilon), Y^\varepsilon(t) = (X_1(t/\varepsilon), \dots, X_d(t/\varepsilon))) :$

	événements	Intensité
self-renew :	$(X, Y) \rightarrow (X + \varepsilon, Y),$	$\frac{1}{\varepsilon} r_0(Y)X,$
activation :	$(X, Y) \rightarrow (X - \varepsilon, Y + e_1),$	$\frac{1}{\varepsilon} \lambda_0(Y)X,$
atresia :	$(X, Y) \rightarrow (X - \varepsilon, Y),$	$\frac{1}{\varepsilon} \mu_0(Y)X,$
growth :	$(X, Y) \rightarrow (X, Y + e_{i+1} - e_i),$	$\frac{1}{\varepsilon} \lambda_i(Y)Y_i, i = 1..d - 1,$
atresia :	$(X, Y) \rightarrow (X, Y - e_i),$	$\frac{1}{\varepsilon} \mu_i(Y)Y_i, i = 1..d,$

	événements	Intensité
self-renew :	$(X, Y) \rightarrow (X + \varepsilon, Y),$	$\frac{1}{\varepsilon} r_0(Y)X,$
activation :	$(X, Y) \rightarrow (X - \varepsilon, Y + e_1),$	$\frac{1}{\varepsilon} \lambda_0(Y)X,$
atresia :	$(X, Y) \rightarrow (X - \varepsilon, Y),$	$\frac{1}{\varepsilon} \mu_0(Y)X,$
growth :	$(X, Y) \rightarrow (X, Y + e_{i+1} - e_i),$	$\frac{1}{\varepsilon} \lambda_i(Y)Y_i, i = 1..d - 1,$
atresia :	$(X, Y) \rightarrow (X, Y - e_i),$	$\frac{1}{\varepsilon} \mu_i(Y)Y_i, i = 1..d,$

Theorem (G. Ballif, F. Clément, R.Y. *en révision*)

(...) $(X^\varepsilon, Y^\varepsilon)$ converge dans $\mathcal{D}_{\mathbb{R}}[0, \infty[\times \mathcal{L}_m(\mathbb{N}^d)$ vers l'unique solution de

$$\begin{cases} \frac{dx}{dt}(t) &= \Lambda_0(x(t))x(t), & x(0) = x^{\text{in}}, \\ \Lambda_0(x(t)) &= \sum_{y \in \mathbb{N}^d} (r_0(y) - \lambda_0(y) - \mu_0(y)) \pi_{x(t)}(y), & \text{où} \end{cases}$$

$$\sum_{y \in \mathbb{N}^d} L_x \psi(y) \pi_x(y) = 0, \quad \forall \psi \text{ borné sur } \mathbb{N}^d,$$

$$L_x \psi(y) = \lambda_0(y)x \left[\psi(y + e_1) - \psi(y) \right] + \sum_{i=1}^{d-1} \lambda_i(y)y_i \left[\psi(y + e_{i+1} - e_i) - \psi(y) \right] \\ + \sum_{i=1}^d \mu_i(y)y_i \left[\psi(y - e_i) - \psi(y) \right].$$

Éléments de preuves

- Estimée sur les moments :

$$\forall p \geq 1, \sup_{\varepsilon} \mathbb{E} \left(\sup_{t \geq 0} \left| X^\varepsilon(t) + \sum_{i=1}^d Y_i^\varepsilon(t) \right|^p \right) < \infty$$

- Identification de la martingale "lente" :

$$M_f^\varepsilon(t) = f(X^\varepsilon(t)) - \int_0^t Af(X^\varepsilon(s), Y^\varepsilon(s)) ds + R_f^\varepsilon(t) \text{ où}$$

$$Af(x, y) = \left(r_0(y) - \lambda_0(y) - \mu_0(y) \right) x f'(x)$$

- Identification de la martingale "rapide" :

$$M_g^\varepsilon(t) := \varepsilon \left[g(Y^\varepsilon(t)) - g(Y^\varepsilon(0)) \right] - \int_0^t \int_{\mathbb{N}^d} L_{X^\varepsilon(s)} g(Y^\varepsilon(s)) ds$$

	événements	Intensité
self-renew :	$(X, Y) \rightarrow (X + \varepsilon, Y),$	$\frac{1}{\varepsilon} r_0(Y)X,$
activation :	$(X, Y) \rightarrow (X - \varepsilon, Y + e_1),$	$\frac{1}{\varepsilon} \lambda_0(Y)X,$
atresia :	$(X, Y) \rightarrow (X - \varepsilon, Y),$	$\frac{1}{\varepsilon} \mu_0(Y)X,$
growth :	$(X, Y) \rightarrow (X, Y + e_{i+1} - e_i),$	$\frac{1}{\varepsilon} \lambda_i(Y)Y_i, i = 1..d - 1,$
atresia :	$(X, Y) \rightarrow (X, Y - e_i),$	$\frac{1}{\varepsilon} \mu_i(Y)Y_i, i = 1..d,$

Hypothèses

- ★ $r_0(y) < R_0, \forall y$
- ★ $\lambda_0(y) \leq B_0, \forall y$
- ★ $\lambda_i(y) > 0, i \in \llbracket 0, d - 1 \rrbracket, \forall y$
- ★ $\mu_d(y) > 0, \forall y$
- ★ $\alpha_i > 0$ tel que $\lambda_i(y) + \mu_i(y) \geq \alpha_i, \forall i \in \llbracket 0, d \rrbracket, \forall y$

Éléments de preuves

- Processus majorant linéaire :

$$\begin{array}{ll}
 (U, V) \rightarrow (U + \varepsilon, V), & \frac{1}{\varepsilon} R_0 U, \\
 (U, V) \rightarrow (U, V + e_1), & \frac{1}{\varepsilon} B_0 U, \\
 (U, V) \rightarrow (U - \varepsilon, V + 1), & \frac{1}{\varepsilon} \alpha_0 U, \\
 (U, V) \rightarrow (U, V + e_{i+1} - e_i), & \frac{1}{\varepsilon} \alpha_i V_i.
 \end{array}$$

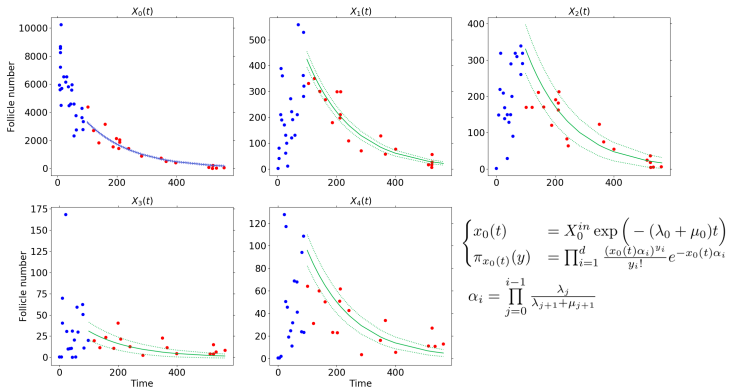
- Par couplage : $X \leq U$ et $\sum_{j=1}^i Y_j \leq \sum_{j=1}^i V_j$.
- Lyapounov $F(y) = \sum_{i=1}^d \left(\sum_{j=1}^i y_j \right)^{p_i}$ pour $p_i \searrow$.

Pour l'unicité :

$$\frac{dx}{dt}(t) = \langle r_0 - \lambda_0 - \mu_0, \pi_{x(t)} \rangle x(t)$$

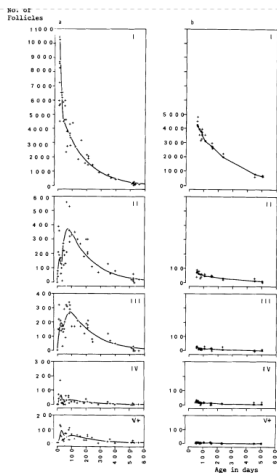
- Lyapounov $F : \langle \pi_x, F \rangle < \infty$.
- Pour toute fonction f tel que $|f| \leq F$
 $\langle f, \pi_x - \pi_{x'} \rangle = (x - x') \langle (g_x(\cdot + 1) - g_x(\cdot)) \lambda_0, \pi_{x'} \rangle$
où g_x est solution de l'équation de Poisson :
 $L_x g_x = \langle f, \pi_x \rangle - f$ et vérifie $|g_x| \leq F$

Modèle limite



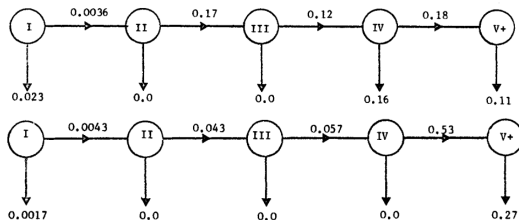
- La séparation de l'échelle de temps est cohérente avec les connaissances biologiques et les données de comptage des follicules.

Modèles de population de follicules (vie reproductive)



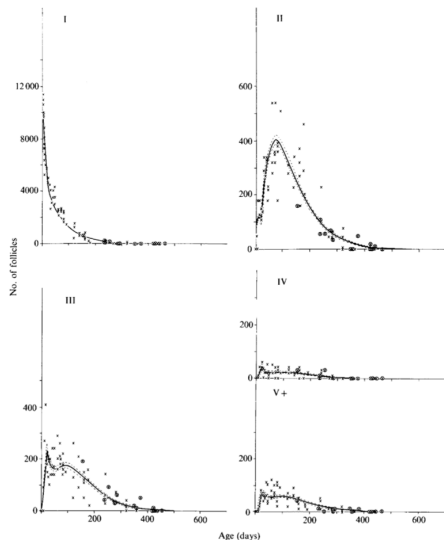
Faddy et al., J. Exp. Zool. 1976

- Peut-on expliquer ces dynamiques avec des interactions non linéaire ?
Comment les analyser sur l'échelle de temps de vie d'un individu ?
- **Quels paramètres peut-on inférer à partir de ces observations ?**
(Preliminary results)



"Time" course

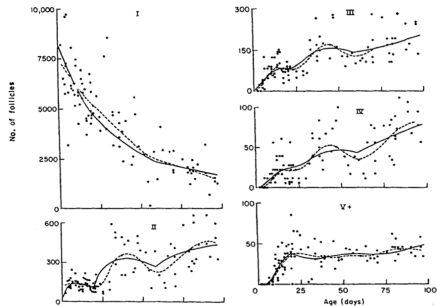
- Follicle count in mice of strain **CBA** from birth until 500 days.
- Reserve + 4 compartments (classification of Faddy)
- (Recovery of points by hand)



Faddy, Gosden and Edwards, J. Endo., 1983

"Time" course

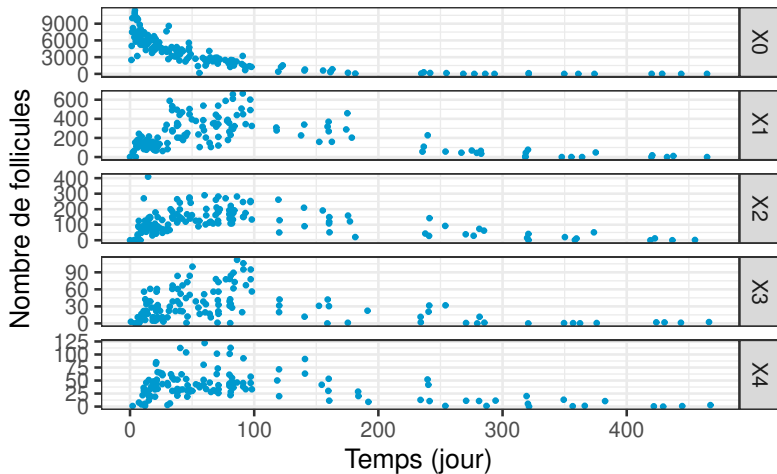
- Follicle count in mice of strain **CBA/CA** from birth until 100 days.
- Reserve + 4 compartments (classification of Faddy)
- (Recovery of points by hand)



Faddy, Telfer and Gosden, Cell Proliferation, 1987

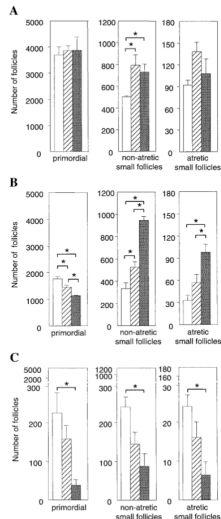
Faddy, Telfer and Gosden, Cell Proliferation, 1987

"Time" course



Perturbation data : KO AMH

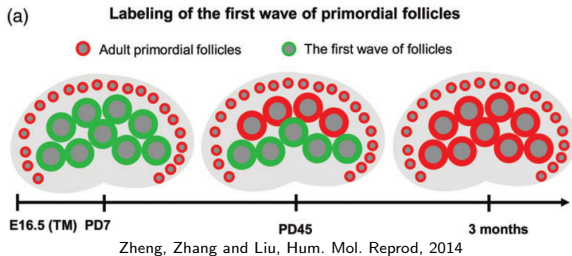
- AMH Inhibition *in vivo* on mice of strain **C57B6**.
- 3 genotypes : control group (+/+), heterozygous mice KO AMH (+/-) homozygous mice KO AMH (-/-).
- Follicle counts at 3 ages :
 - 25 days (A)
 - 120 days (B)
 - 390 days (C)



Durlinger and al, Endocrinology, 1999

Refinement on "initial" condition

- Two distinct population of follicles are present initially
- Labelling of each population

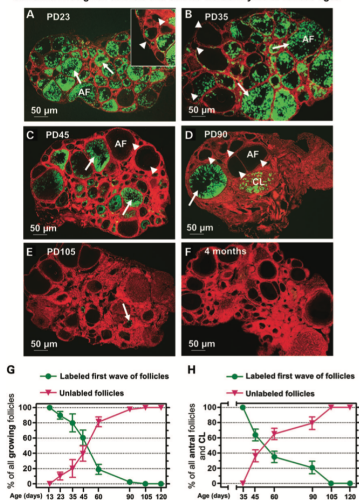


Refinement on "initial" condition

- Tracing follicles of the first wave of activated follicles (in green).
- Proportion $p(t)$ of first wave activated follicles among growing follicles.

$$p(t) = \frac{\sum_{i=1}^4 X_i^1(t)}{\sum_{i=1}^4 X_i^{tot}(t)}$$

Tamoxifen was given at E16.5 and ovaries were analyzed at various ages



Zheng, Zhang and al, Hum. Mol. Gen, 2014

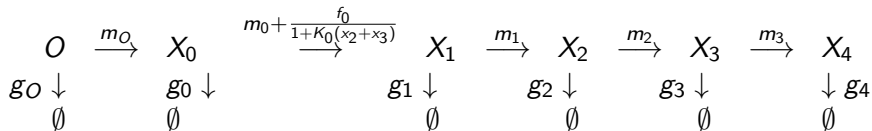
EDO model

O = germ cell before entering in follicle (pre/peri-natal)

X_i = Follicle in maturity stage i

$O + O$

$\uparrow r_0$

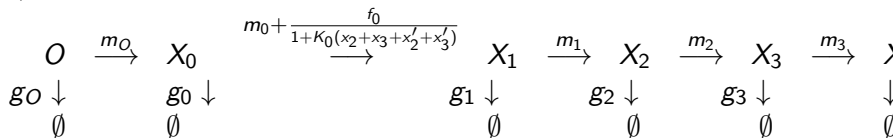


EDO model

2 populations (O, X_i) and (O', X'_i) :

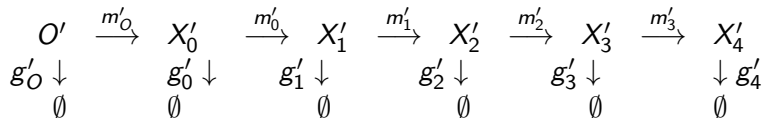
$O + O$

$\uparrow r_O$



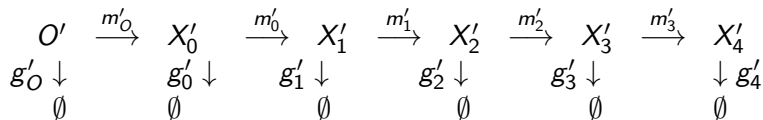
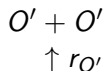
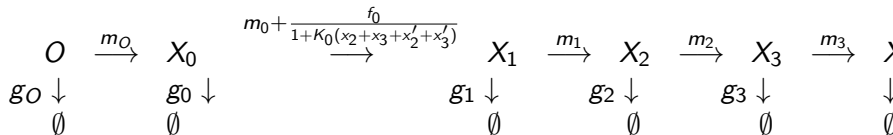
$O' + O'$

$\uparrow r_{O'}$



EDO model

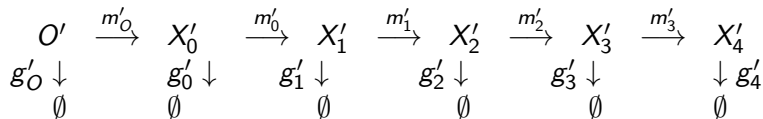
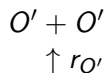
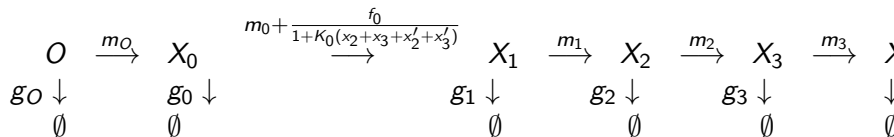
2 populations (O, X_i) and (O', X'_i) :



K_0 AMH : $K_0 = 0$

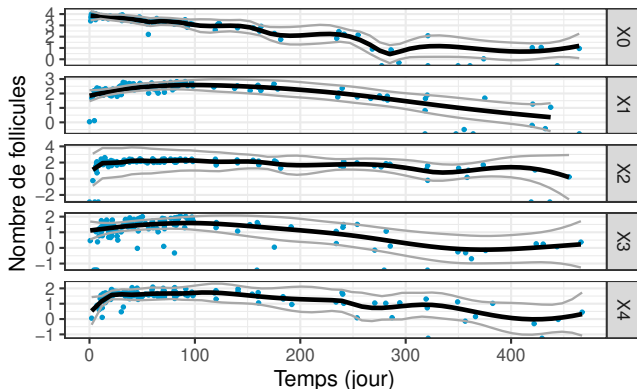
EDO model

2 populations (O, X_i) and (O', X'_i) :



27 paramètres...

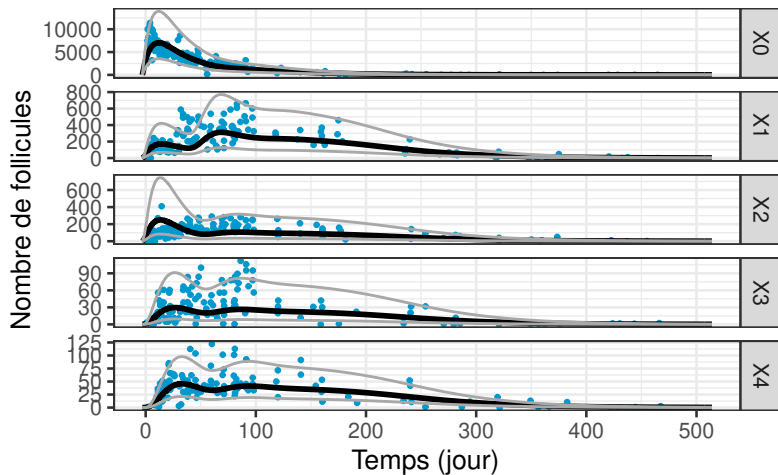
Cost function



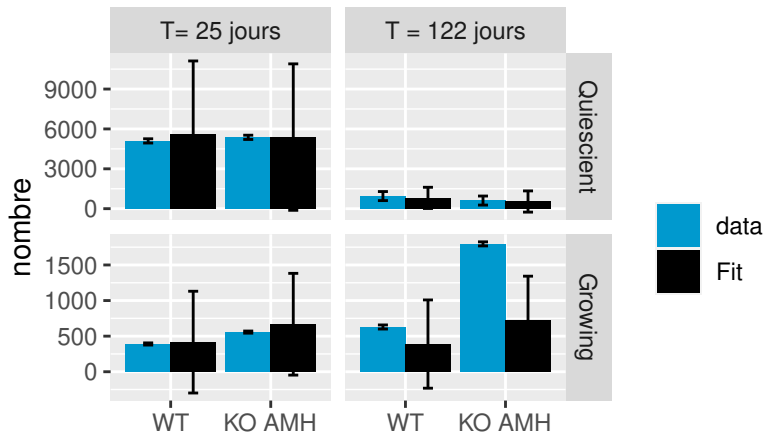
Multiplicative lognormal statistical model :

$$J_{faddy}(\theta) = \sum_{j=0}^4 \left[\frac{1}{M_j} \sum_{i=1}^{M_j} \left(\frac{\log(x_0^\theta(t_i^0)) - \log(x_i^0)}{\sigma_j} \right)^2 + \log(\sigma_j) \right]$$

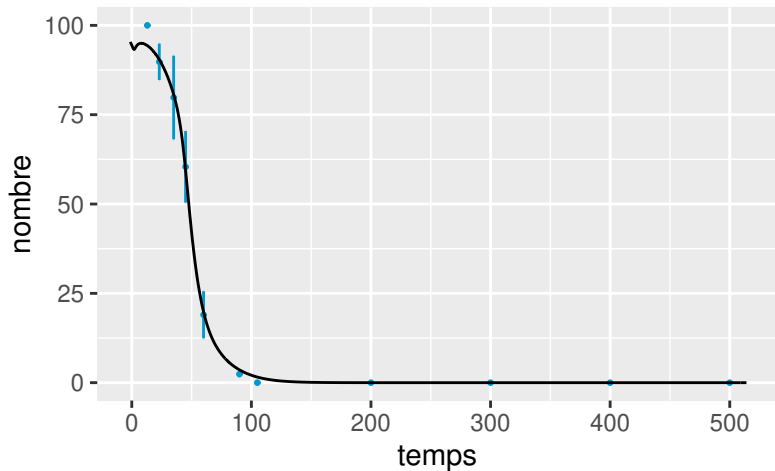
Data fitting



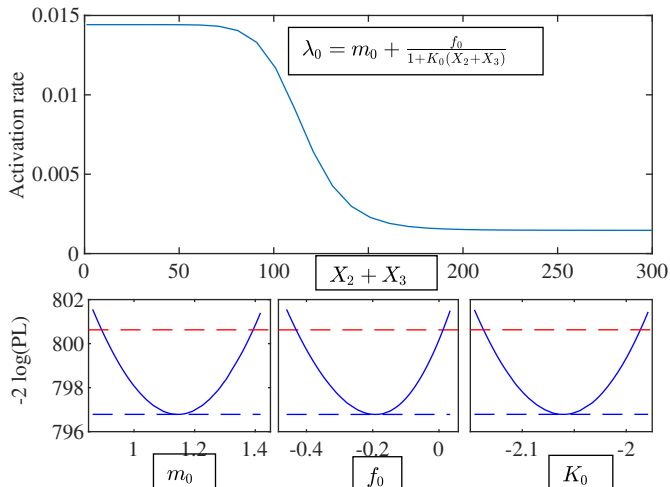
Data fitting



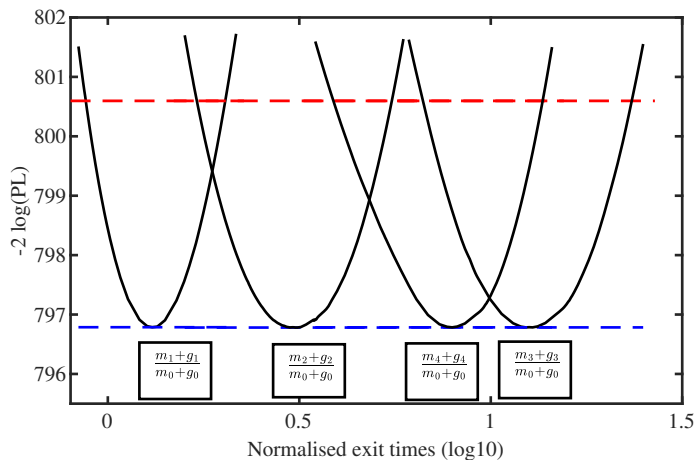
Data fitting



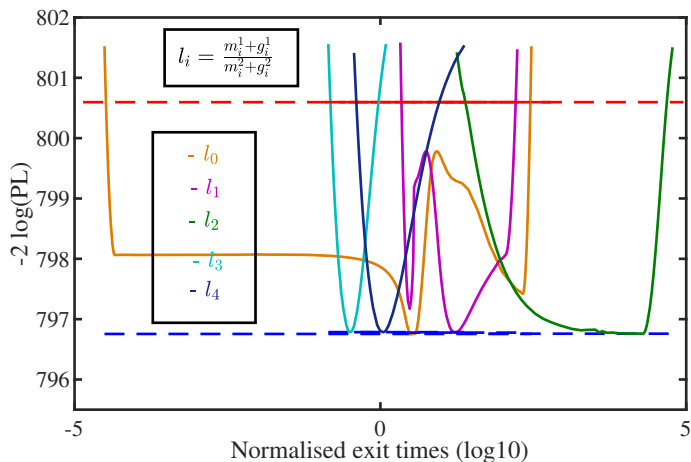
Taux d'activation



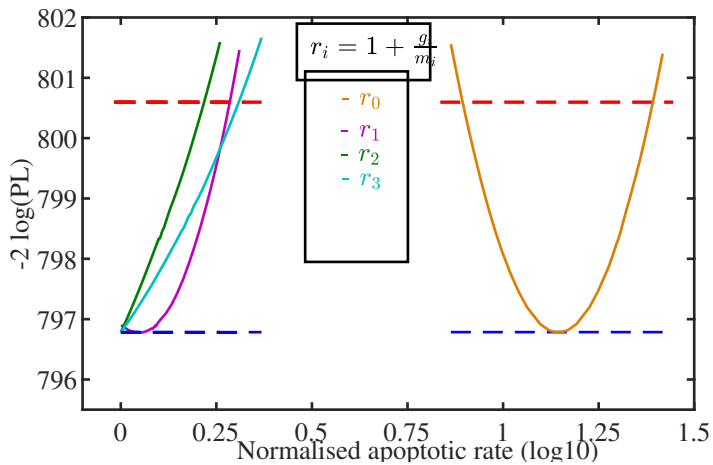
Vitesse d'évolution follicules en croissance / quiescent



Comparaison 1er/2e vague

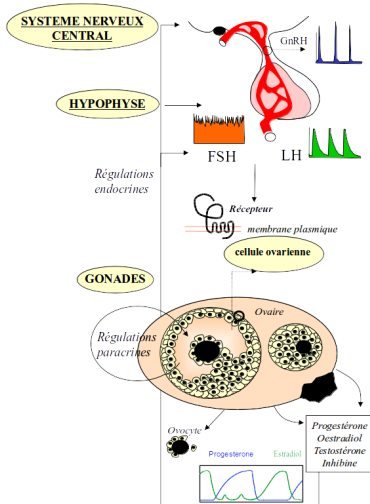


Taux d'atrésie



Le système reproducteur féminin des mammifères : un système multi-échelle complexe

- **Signaux neuro-hormonaux**
Encodage et décodage
- **Gamétogenèse**
Dynamique de population
- **Croissance d'un follicule**
Morphodynamique de cellules
- **Niveau intra-cellulaire**
réseaux de signalisation



R.Y., P. Crépieux, E. Reiter, A. Poupon, F. Clément, *Advances in computational modeling approaches of pituitary gonadotropin signaling*, Expert Opinion on Drug Discovery, 2018.



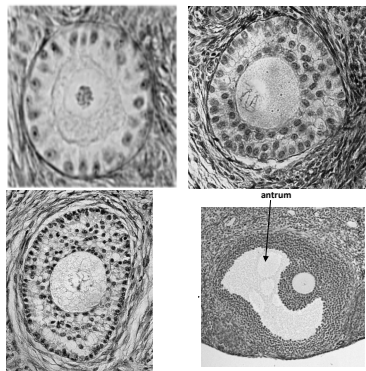
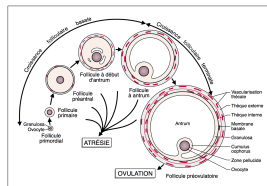
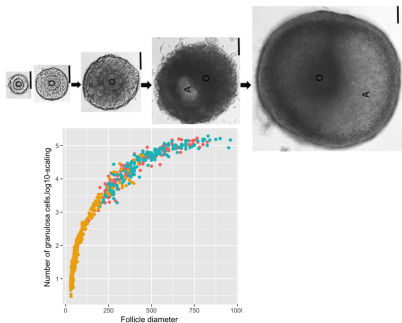
F. Clément, P. Crépieux, R. Y., and D. Monniaux. Mathematical modeling approaches of cellular endocrinology within the hypothalamo-pituitary-gonadal axis. *Mol. Cell. Endocrinol.* 2020.

Le système reproducteur féminin des mammifères : un système multi-échelle complexe

- **Croissance d'un follicule**

Morphodynamique de population

- Espace : niveau cellulaire
- Temps : Plusieurs cycles ovariens



Courtesy of Danielle Monniaux.



Key features of follicle initiation

- Leave the **quiescent** phase (static reserve)
- A single layer of somatic cells
- **Two types** of cells : Flattened and Cuboid
- **Irreversible transition** from Flattened to Cuboid cells
- The follicle is "activated" when all cells have transitioned
- **"Awakening"** signals both from external and internal cues

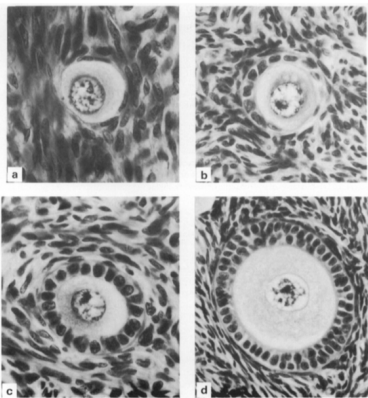
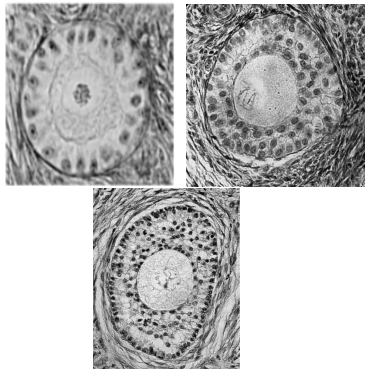


Fig. 1. Illustrations of follicle types: (a) Type B, $\times 570$; (b) Type B/C, $\times 570$; (c) Type C, $\times 570$; (d) Type D, $\times 410$.

Gougeon & Chainy, J. Reprod. Fert. 1987

Key features of follicle basal growth

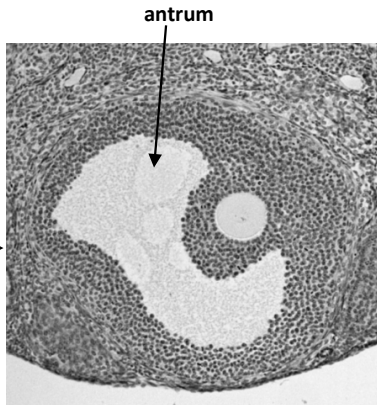
- Growth of a small follicle after initiation
- **Spherical Symmetry**
- Spatial structure of somatic cells in concentric **layers**
- Joint dynamic
 - ★ Ovocyte **growth**
 - ★ Somatic cells **Proliferation**
- Growth signals from the Ovocyte to somatic cells and *vice-versa*.



Courtesy of Danielle Monniaux.

Key features of Follicle terminal growth

- Lost of spherical symmetry
- Joint Dynamic
 - ★ Liquid-filled cavity formation and growth
 - ★ Switch from proliferation to differentiation of somatic cells
 - ★ Morphogen gradient
- **Role of the Liquid-filled cavity ?**



Tertiary (antral) follicle

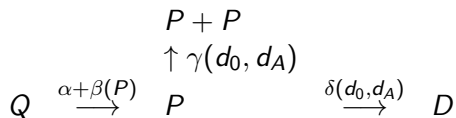
EDO model

Q = Quiescent cells

P = Proliferative cells

D = Differentiated cells

d_0, d_A = germ cell and antrum diameters



$$\frac{d}{dt}d_0 = f(d_0, P)$$

$$\frac{d}{dt}d_A = g(d_A, P, Q)$$

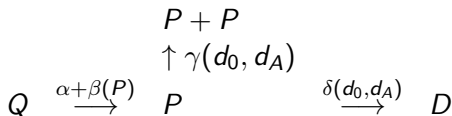
EDO model

Q = Quiescent cells

P = Proliferative cells

D = Differentiated cells

d_O, d_A = germ cell and antrum diameters

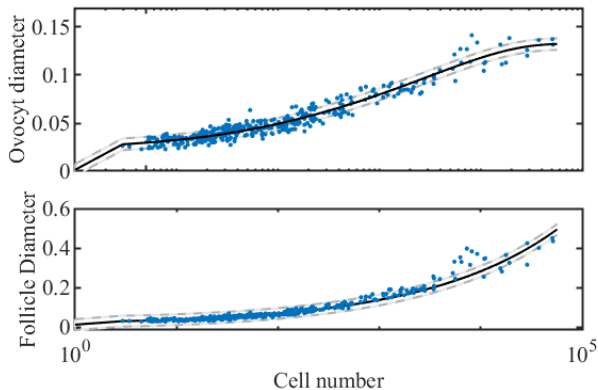


$$\frac{d}{dt}d_0 = f(d_0, P)$$

$$\frac{d}{dt}d_A = g(d_A, P, Q)$$

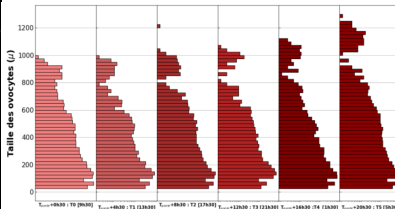
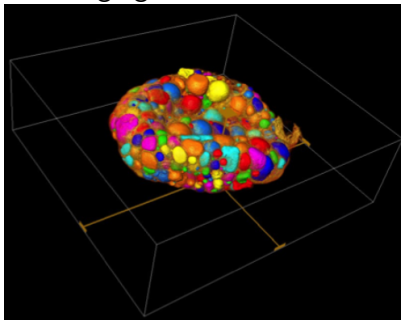
β, γ, δ, f and g depends on various functional hypotheses of molecular dialogue inside a follicle.

Data fitting



- ✓ data fitting shows (or confirms) positive feedback loop for Quiescent cells activation (through Proliferative cells), germ cell growth (through Proliferative cells) and antrum growth (through Proliferative/Differentiative cells)

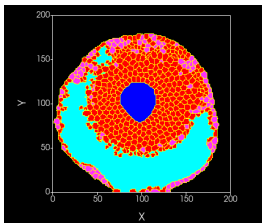
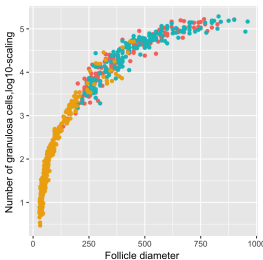
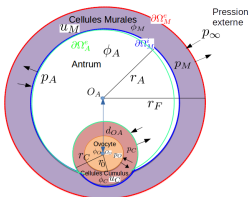
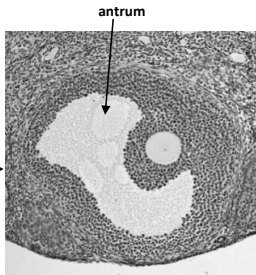
3D imaging data : Follicle count and morphometric measurement



-> structuring the population based on morphologic variable.

$$\begin{cases} \frac{d\rho_0(t)}{dt} & = -(\lambda_0(\rho(t, \cdot)) + \mu_0(\rho(t, \cdot)))\rho_0(t), \\ \varepsilon \partial_t \rho(t, x) & = -\partial_x (\lambda(\rho(t, \cdot), x)\rho(t, x)) - \mu(\rho(t, \cdot), x)\rho(t, x), \\ \lim_{x \rightarrow 0} \lambda(\rho(t, \cdot), x)\rho(t, x) & = \lambda_0(\rho(t, \cdot))\rho_0(t), \end{cases}$$

Vers des modèles plus réalistes ? Croissance antrale



work in progress...

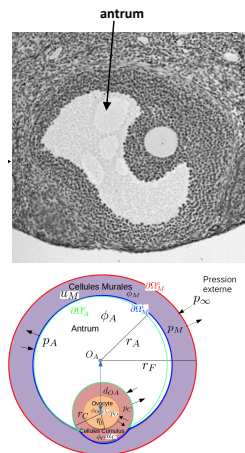


Antrum growth model

- Multiphasic advection-diffusion-reaction PDE

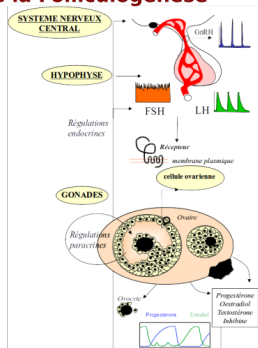
$$\begin{aligned}
 (\partial_t + \text{div}_x(v_M \cdot)) u_M &= R_M \\
 v_M &= -\mu_M \nabla_x p_M, \\
 p_M &= C_M (u_M - u_0)^{\gamma_M}, \\
 (\partial_t + \text{div}_x(v_a \cdot)) \Phi_a &= D \Delta \Phi_a + R_a \\
 \text{div}_x v_a &= 0, \\
 \nabla \Phi_a \cdot \vec{n}_a &= s(t) = \kappa \int_{\Omega_M} u_M(t, x) dx \\
 \frac{d}{dt} \left(\frac{4}{3} \pi r_a(t)^3 \right) &= J_{H_2O} = L_p(t) (\Delta \Pi - \Delta p) \\
 \Delta \Pi &= c_a \Phi_a^{\gamma_a} \\
 \Delta p &= p_M(t, |x| = r_a^+) - p_e \\
 L_p(t) &= \frac{\Pi(r_F(t) - r_a(t))^4}{8\eta\epsilon(u_M)} n(u_M),
 \end{aligned}$$

+ Boundary conditions and constitutive laws
work in progress with Erwan Hingant...



Merci de votre attention !

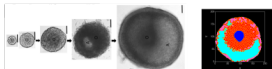
Modélisation Multi-échelle de la Folliculogénèse



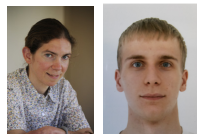
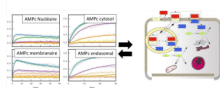
Echelle tissulaire



Echelle cellulaire



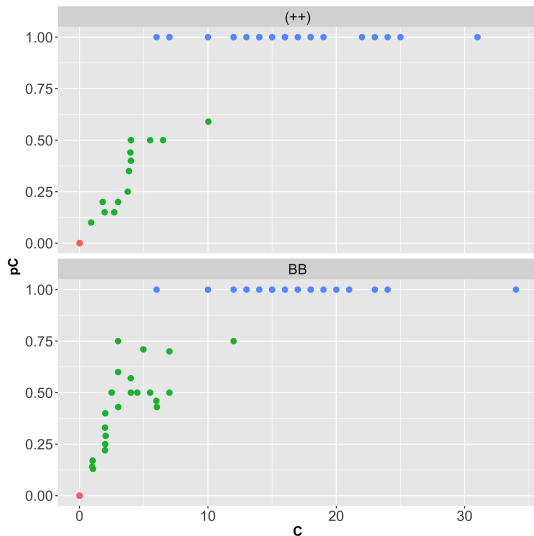
Echelle intra-cellulaire



Inria INRAE

- ★ INRIA Saclay : Frédérique Clément, Guillaume Ballif, Frédérique Robin
- ★ INRAE PRC : Team BIOS, BINGO (Danielle Monniaux, Véronique Cadoret, Rozenn Dalbies-Tran)
- ★ INRAE LPGP (Julien Bobe, Violette Themes)
- ★ CEMRACS 2018 (Céline Bonnet, Keltoum Chahour)

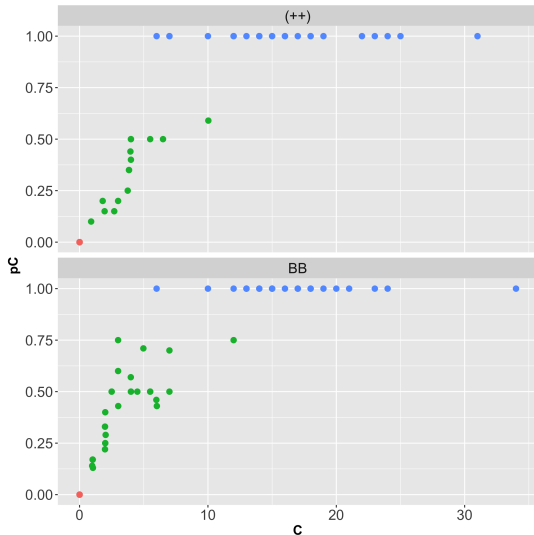
Ex vivo data (snapshot data)



- Ex vivo data in sheep fetus (Courtesy of K. McNatty) : WT (++) vs Mutant (BB)

⇒ **Proportion of cuboid cells**
 $p_C = C/(F + C)$ vs **number of cuboid cells C**

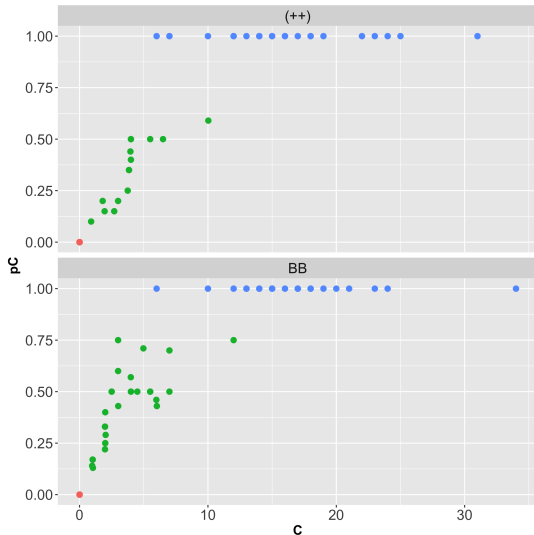
Ex vivo data (snapshot data)



- Ex vivo data in sheep fetus WT vs BB
- Once activated, follicles have "fast" cell proliferation

⇒ **Are both differentiation et de proliferation process concomitant or successive ?**

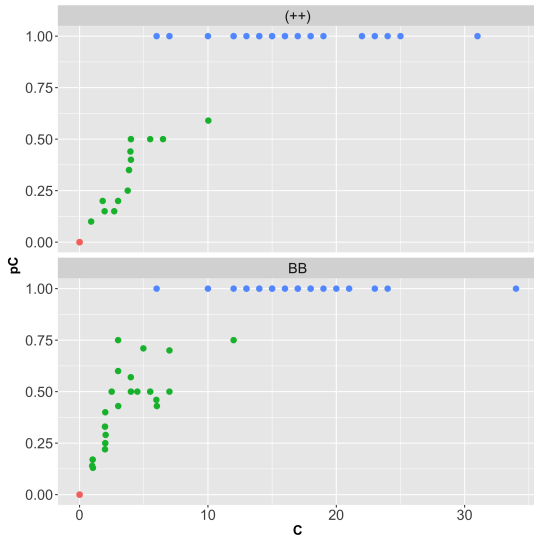
Ex vivo data (snapshot data)



- Ex vivo data in sheep fetus WT vs BB
- Proportion of cuboid cells seems higher in mutant than WT, for a given number of cuboid cells.

⇒ **Is it coming from a kinetic difference?**

Ex vivo data (snapshot data)



- Ex vivo data in sheep fetus WT vs BB
- Regulatory mechanism for this process are barely known.

⇒ **Is the transition of cell differentiation abrupt or more progressive ?**

Events	Reaction	Intensity function
differentiation	$F \rightarrow C$	$\alpha F + \beta \frac{FC}{F+C}$
prolifération	$C \rightarrow C + C$	γC

- ↪ Two cell populations : F (flattened) and C (cuboid)
- ↪ Small number of cells
- ↪ Retro-action of cuboid cells on the differentiation rate : is it relevant ?
- ↪ From $(F_0, 0)$ to $(0, C_\tau)$

- Theoretical study

⇒ Statistics of the "transition" time τ to reach $F = 0$.

⇒ Variability of final cuboid cells ($\mathbb{E}[C_\tau] < \infty$ if $\gamma < \alpha + \beta$)

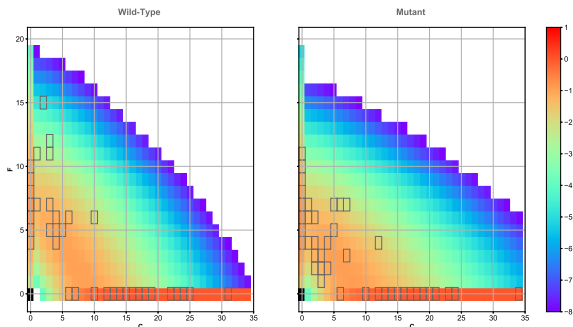
⇒ Impact of parameters e.g. on qualitative dynamics
(progressive vs abrupt)

- Parameter calibration : lack of identifiability. Either $\gamma \ll 1$ and β unconstrained, or $\gamma > 1$ and $\beta/\gamma \gg 1$



Robin et al. *Stochastic nonlinear model for somatic cell population dynamics during ovarian follicle activation*, (submitted) arXiv :1903.01316

Agreement to data



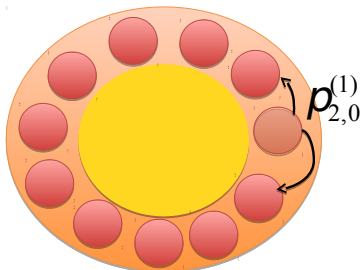
- ⇒ The model can capture both data sets
- ⇒ Lack of identifiability (non-conclusive on retro-action)
- ⇒ First differentiation, then proliferation (slightly more concomitant in mutant case)



Robin et al. *Stochastic nonlinear model for somatic cell population dynamics during ovarian follicle activation*, (submitted) arXiv :1903.01316

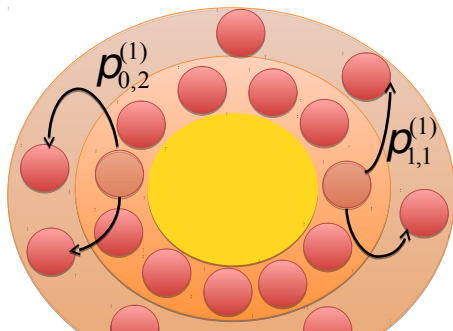
Dynamical model (Multi-type Bellman-Harris Branching process)

- **Age** and **position** dependent division rate (cell cycle regulated by the ovocyte)
- At division, unidirectional motion **centrifugal**
- Cells are **independent** between each other (Unlimited layer capacity)



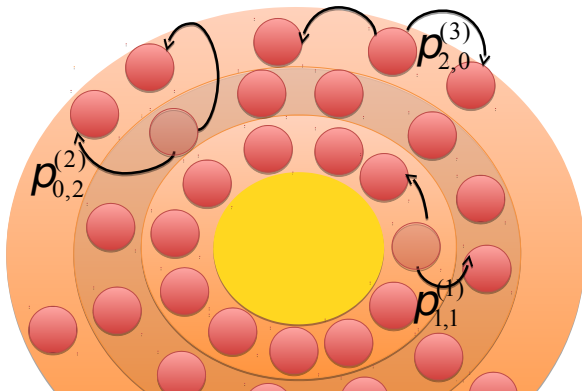
Dynamical model (Multi-type Bellman-Harris Branching process)

- **Age** and **position** dependent division rate (cell cycle regulated by the ovocyte)
- At division, unidirectional motion **centrifugal**
- Cells are **independent** between each other (Unlimited layer capacity)



Dynamical model (Multi-type Bellman-Harris Branching process)

- **Age** and **position** dependent division rate (cell cycle regulated by the ovocyte)
- At division, unidirectional motion **centrifugal**
- Cells are **independent** between each other (Unlimited layer capacity)



Data

- We have counting data of somatic cells in snapshot data, morphological data (diameter) and *order of magnitude of transit times between follicle "type"*

	$t = 0$	$t = 20$	$t = 35$
#Data points	34	10	18
Total cell number	113.89 ± 57.76	885.75 ± 380.89	2241.75 ± 786.26
Oocyte diameter (μm)	49.31 ± 8.15	75.94 ± 10.89	88.08 ± 7.43
Follicle diameter (μm)	71.68 ± 13.36	141.59 ± 17.11	195.36 ± 23.95

Data

- We have counting data of somatic cells in snapshot data, morphological data (diameter) and *order of magnitude of transit times between follicle "type"*

	$t = 0$	$t = 20$	$t = 35$
#Data points	34	10	18
Total cell number	113.89 ± 57.76	885.75 ± 380.89	2241.75 ± 786.26
Oocyte diameter (μm)	49.31 ± 8.15	75.94 ± 10.89	88.08 ± 7.43
Follicle diameter (μm)	71.68 ± 13.36	141.59 ± 17.11	195.36 ± 23.95

⇒ Can we explain proliferation in concentric layers by a simple model of "division-migration"? Or do physical constraint play important role?

Data

- We have counting data of somatic cells in snapshot data, morphological data (diameter) and *order of magnitude of transit times between follicle "type"*

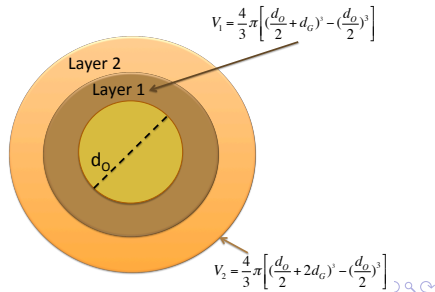
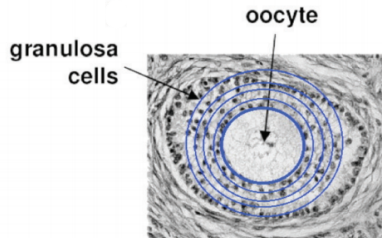
	$t = 0$	$t = 20$	$t = 35$
#Data points	34	10	18
Total cell number	113.89 ± 57.76	885.75 ± 380.89	2241.75 ± 786.26
Oocyte diameter (μm)	49.31 ± 8.15	75.94 ± 10.89	88.08 ± 7.43
Follicle diameter (μm)	71.68 ± 13.36	141.59 ± 17.11	195.36 ± 23.95

- ⇒ Can we characterize the growth rate of a follicle and spatial repartition of somatic cells ?
- ⇒ What is the impact of spatial position of a somatic cell on its division rate ?

Simple model : spatial compartment in successive layers

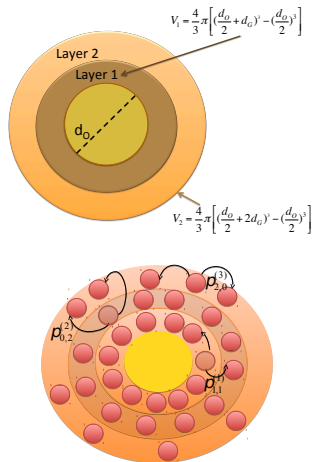
- Spherical ovocyte (d_o)
- Linear proliferation dynamics of somatics cells
- Layer dependent division rate
- Multi-type Bellman-Harris Branching process

Somatic cells divide and migrate to successive layers.



- The geometrical model allows a simple spatial description
- The model is linear and decomposable : **exponential growth**, with a stable asymptotic spatial profile : there exists a unique $\lambda > 0$ such that the process Z_t verifies

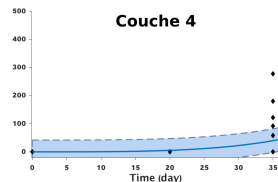
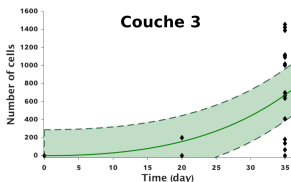
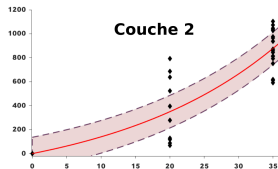
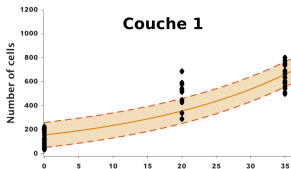
$$\lim_{t \rightarrow \infty} Z_t e^{-\lambda t} = \hat{Z} \quad (\text{in law})$$



Clément et al. *Analysis and Calibration of a Linear Model for Structured Cell Populations with Unidirectional Motion : Application to the Morphogenesis of Ovarian Follicles*, SIAM App. math, 2019

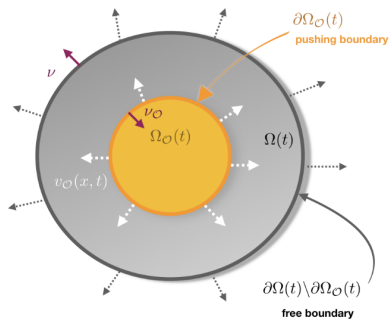
Fitting results

- ⇒ **Exponential** growth dominated by the first cell layer
- ⇒ Parameter identifiability and doubling time quantification (≈ 16 days) :
Cell-cycle time ↗ with ovocyte distance



Clément et al. *Analysis and Calibration of a Linear Model for Structured Cell Populations with Unidirectional Motion : Application to the Morphogenesis of Ovarian Follicles*, SIAM App. math, 2019

More realistic model ?



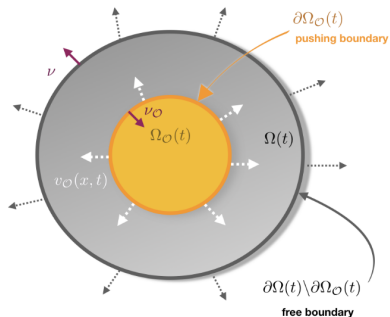
$\frac{\partial u}{\partial t} + \text{div}(\vec{\nabla} u) = b(x)u(t, x)$
 for $x \in \Omega(t)$ and with $\vec{\nabla}$ linked
 to the negative gradient of the
 pressure, and the pressure related
 to the density...

Under locally constant density
 and spherical geometry, one
 have :

$$\frac{d}{dt}(r_F(t)) = \gamma \int_{\Omega(t)} b(x) dx + \frac{d}{dt}(r_O(t))$$

work in progress...

Vers des modèles plus réalistes ?



- Advection-reaction PDE

$$\frac{\partial u}{\partial t} + \operatorname{div}(\vec{V}u) = b(x)u(t, x)$$

$$\vec{V} \sim \nabla u$$

$$\frac{d}{dt}(r_F(t)) = \gamma \int_{\Omega(t)} b(x) dx + \frac{d}{dt}(r_O(t))$$

work in progress...

The Mammalian female reproductive system : a complex multiscale system

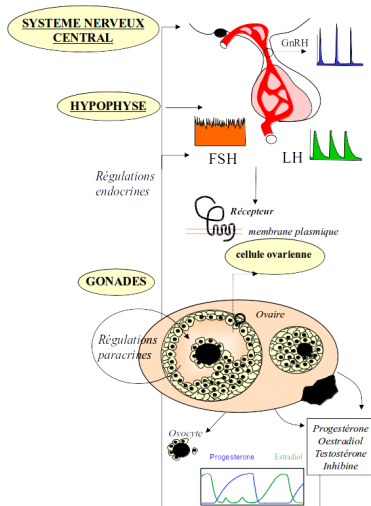
Encoding and decoding **neuro-hormonal signals**

Population dynamics : **gametogenesis**

Intra-cellular level : **signaling networks**

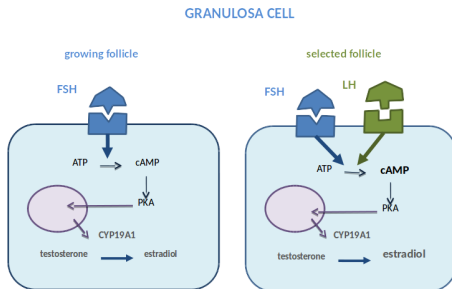


Yvinec et al., *Advances in computational modeling approaches of pituitary gonadotropin signaling*, Expert Opinion on Drug Discovery, 2018.



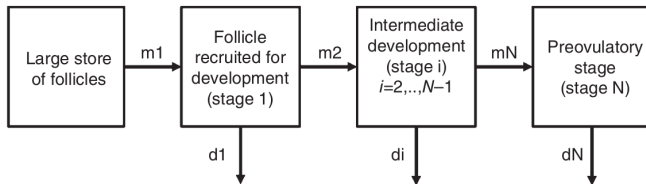
cAMP-induced FSH and its regulation at the cellular level

- FSHR signaling network and short-term cAMP induction.
 - Long-term regulation of the FSHR network during follicular selection.
- ⇒ The Cellular "switch" is a pre-requisite for follicle selection .
- ⇒ This switch is implemented at molecular level by the FSHR network and cAMP output (which is a good marker of follicle maturity).



Summary

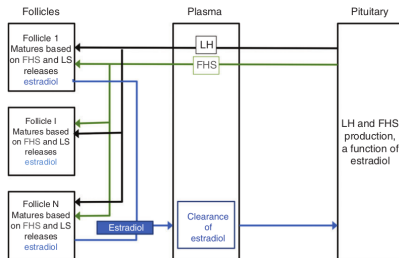
- Circulating hormones dynamical models (Selgrade's model)
- Follicles dynamics in compartment (Faddy's model)
 - ★ Reproductive lifespan timescale
 - ★ Follicle communication and "hormonal control" through population feedback



Clark & Kruger, WIREs Syst Biol Med 2017

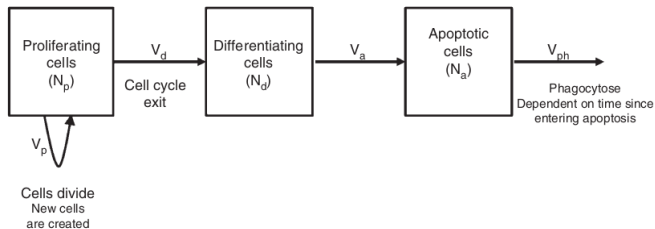
Summary

- Circulating hormones dynamical models (Selgrade's model)
- Follicles dynamics in compartment (Faddy's model)
- Coupled Hormonal/Follicle dynamical models (Lacker's & Clément's model)
 - ★ Ovarian cycle / follicle cohort timescale
 - ★ Follicle cohort subject to a shared hormonal environment
 - ★ The individual follicle maturity rate has local positive feedback and global negative feedback.



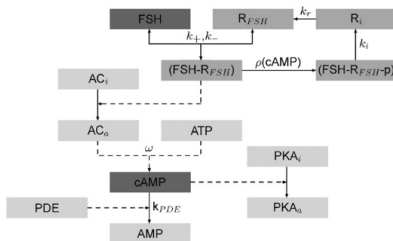
Summary

- Circulating hormones dynamical models (Selgrade's model)
- Follicles dynamics in compartment (Faddy's model)
- Coupled Hormonal/Follicle dynamical models (Lacker's & Clément's model)
- Cell dynamics in a single follicle (Clément's model)
 - ★ Cell cycle time scale
 - ★ Pool of different cell types within a single follicle
 - ★ Complex geometry and moving boundary problems



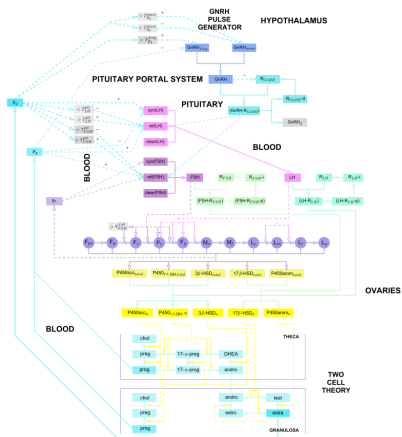
Summary

- Circulating hormones dynamical models (Selgrade's model)
- Follicles dynamics in compartment (Faddy's model)
- Coupled Hormonal/Follicle dynamical models (Lacker's & Clément's model)
- Cell dynamics in a single follicle (Clément's model)
- Intra-cellular dynamics (Clément / Quignot & Bois)
 - ★ Steroidogenesis, cAMP response



Multiscale Models of ovarian follicle selection

- Putting "many" pieces together (Reinecke & Deuflhard)



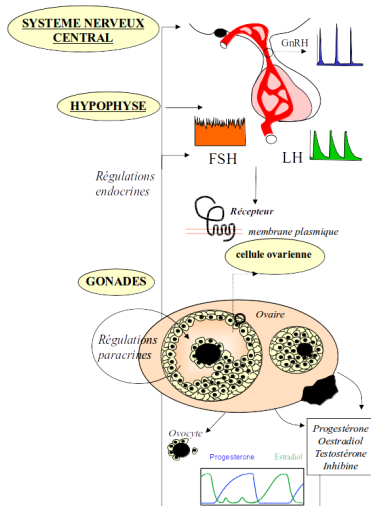
Reinecke & Deuflhard, JTB 2007

- ★ From (stochastic) GnRH pulse generator to detailed steroid metabolism through (compartment-based) follicle development
- ★ *Focus in this paper is on the model development*
- ★ 43 equations (stochastic input and delay differential equations), 191 parameters.

Summary

Population dynamics in ovarian folliculogenesis

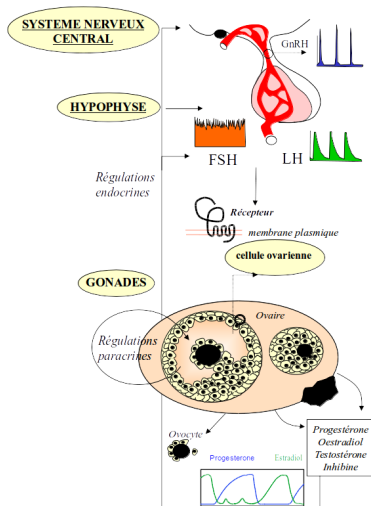
- Somatic cells proliferation, differentiation, and migration during follicle initiation & growth
- Multiscale nonlinear dynamics shape the follicle population distribution into different maturity stages.



Summary

Population dynamics in ovarian folliculogenesis

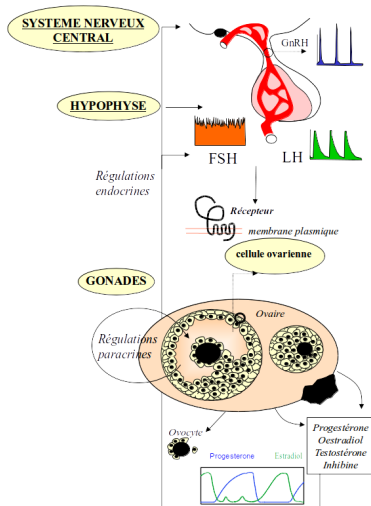
- Somatic cells proliferation, differentiation, and migration during follicle initiation & growth
- Multiscale nonlinear dynamics shape the follicle population distribution into different maturity stages.



Thank you for your attention !

Le système reproducteur féminin des mammifères : un système multi-échelle complexe

- **Signaux neuro-hormonaux**
Encodage et décodage
- **Gamétogenèse**
Dynamique de population
- **Croissance d'un follicule**
Morphodynamique de cellules
- **Niveau intra-cellulaire**
réseaux de signalisation



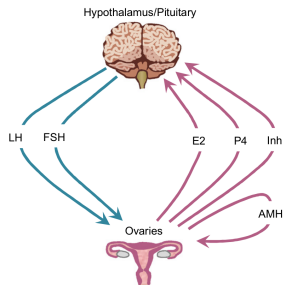
R.Y., P. Crépieux, E. Reiter, A. Poupon, F. Clément, *Advances in computational modeling approaches of pituitary gonadotropin signaling*, Expert Opinion on Drug Discovery, 2018.



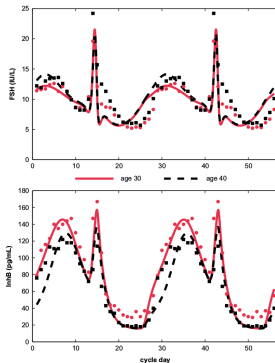
F. Clément, P. Crépieux, R. Y., and D. Monniaux. Mathematical modeling approaches of cellular endocrinology within the hypothalamo-pituitary-gonadal axis. *Mol. Cell. Endocrinol.* 2020.

Neuro-hormonal signals (at the anatomic scale)

Mostly phenomenological equations (DDEs/SDEs) to represent measured levels of circulating hormones, on a daily basis.



Margolskee & Selgrade, JTB 2013

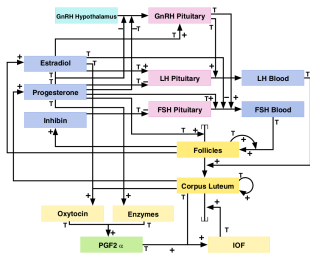


Margolskee & Selgrade, JTB 2013

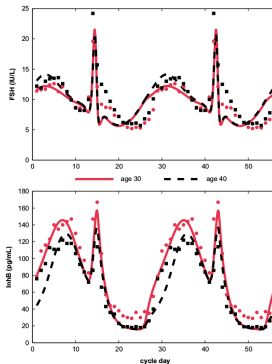
These models can explain some disorders in hormonal levels and predict the effect of pharmaceutical intervention.

Neuro-hormonal signals (at the anatomic scale)

Mostly phenomenological equations (DDEs/SDEs) to represent measured levels of circulating hormones, on a daily basis.



Stötzel et al., *Therio*. 2012



Margolskee & Selgrade, *JTB* 2013

These models can explain some disorders in hormonal levels and predict the effect of pharmaceutical intervention. **Theoretical analysis gets rapidly challenging!**